

# The Calculation of the Effective Tensor Coefficient of the Medium for the Objects with Microinclusions

Ella P. Shurina<sup>1,2</sup>, Mikhail I. Epov<sup>1</sup>, Nadejda V. Shtabel<sup>1</sup>, Ekaterina I. Mikhaylova<sup>1,2</sup>

<sup>1</sup>A.A. Trofimuk Institute of Petroleum Geology and Geophysics SB RAS, Novosibirsk, Russia

<sup>2</sup>Department of Computational Technologies, Novosibirsk State Technical University, Novosibirsk, Russia

Email: [shurina@online.sinor.ru](mailto:shurina@online.sinor.ru)

Received 25 December 2013; revised 25 January 2014; accepted 4 February 2014

Copyright © 2014 by authors and Scientific Research Publishing Inc.

This work is licensed under the Creative Commons Attribution International License (CC BY).

<http://creativecommons.org/licenses/by/4.0/>



Open Access

---

## Abstract

In this paper, several approaches for calculation of the effective tensor coefficient for domains with inclusions have been proposed. The limits of the approaches using are found. The series of numerical experiments are made on the different frequencies, for different inclusions location and boundary conditions for the contrast properties of the matrix and inclusion materials.

## Keywords

Composite Materials; Effective Tensor Coefficient; Vector Finite Element Method

---

## 1. Introduction

The composite materials with microinclusions can be made from dielectric or conductive elements and have the periodical or arbitrary structure. The form of the microinclusions can vary from simple sphere to complex geometry [1]-[3].

The research of the composite materials by analytical methods is quite difficult because of complex geometry and structure of the objects, wide frequency bandwidth and different physical properties of the materials. The classical averaging doesn't lead to physically well-founded results in most cases. Sometimes we can't use these methods at all. We propose to use the numerical modeling methods in this work.

The most effective method for the 3D modeling of the electromagnetic fields is the vector finite element method [4] [5]. In recent years, the special modifications of the finite element method have been done. These modifications are adopted for the modeling electromagnetic field in the media with multiscale and small inclusions. The examples of such methods are the multiscale methods, discontinuous Galerkin method [6] [7].

It should be said that the electrophysical properties of the material with microinclusions can be greatly distinguished from the properties of the source materials. The properties of the composite material are mostly defined by interactions between inclusions. The effective characteristic of the media with the microinclusions can be used when the size of the inclusions is much smaller than the wavelength of the generating field [2] [8] [9]. The popular models of the composite materials in frequency domain are Drude and Lorentz models [2] [3] [8].

Hashin and Shtrikman [10] proposed the variational procedure for the calculation of the effective tensor of conductivity at heterogeneous media with microstructure in 1962. The equivalent parameter of the homogeneous medium lies in the base of this procedure. The electric potential of the medium surface is kept on by using equivalent parameter. Such approach is widely used in the conduction and elasticity problems [9] [11].

We propose to present the composite material with microinclusions as some anisotropic medium. There are some reasons of the anisotropic properties. The material can be isotropic, uniaxial or fully anisotropic, *i.e.* has different properties along different directions. It depends on the type of the relations between molecules of the material. The anisotropy of the dielectric properties of the medium determines by the structure of the lattice [12]. In geophysics the term macroanisotropy is used for the media consists of many small objects [13]-[15]. It can be thin-layered structures, rocks with cracks and pores filled by liquid. Such media can be considered as macroanisotropic without concentrating on the interior media structure [16] [17].

The new approach to the calculation of the effective tensor (anisotropic) characteristic of the medium with microinclusions is proposed in this work. We investigate electromagnetic field in the media with small inclusions. The calculations were made for different frequencies, electrophysical properties of the materials, geometry structure of the researched objects. The effective characteristic of the medium as a complex valued second rank tensor is computed using the results of the 3D modeling of the electromagnetic fields in the medium with microinclusions. The modeling of the electromagnetic field with effective characteristic was done. We compare these results with the results of the modeling in isotropic medium with inclusions.

In Section 2, the variational formulations for modeling of electromagnetic field in the isotropic medium with inclusions and anisotropic medium with effective tensor coefficient are done. The new approach to the calculation of the effective tensor coefficient from the modeling results is described in the Section 3. In Section 4, we compare the results of the computation of the electromagnetic field in the media with inclusions and tensor coefficient. The computations were done on low and high frequencies for different type of field source.

## 2. The Problem Formulation

The electromagnetic field in frequency domain is described by the vector Helmholtz equation with complex valued  $\mathbf{E}$ :

$$\operatorname{curl} \mu^{-1} \operatorname{curl} \mathbf{E} + k^2 \mathbf{E} = 0 \quad \text{in } \Omega \quad (1)$$

where  $\mathbf{E}$  is the electric field (V/m),  $k^2 = i\omega\sigma - \omega^2\varepsilon$  is the wave number;  $\omega = 2\pi f$  is the cyclic frequency [Hz];  $\varepsilon = \varepsilon_r \varepsilon_0$  is the dielectric permittivity [F/m],  $\varepsilon_r$  is the relative dielectric permittivity,  $\varepsilon_0 = 8.85 \times 10E - 12$  F/m;  $\mu = \mu_r \mu_0$  is the magnetic permeability [H/m],  $\mu_r$  is the relative magnetic permeability,  $\mu_0 = 4\pi \times 10E - 7$  H/m;  $\sigma$  is the electric conductivity [S/m] (Figure 1).

The boundary conditions are the following:

$$\mathbf{n} \times \mathbf{E} \Big|_{\Gamma_e} = \mathbf{E}_0, \quad (2)$$

$$\mu^{-1} \operatorname{curl} \mathbf{E} \times \mathbf{n} \Big|_{\Gamma_m} = 0, \quad (3)$$

where  $\Omega \subset \mathbb{R}^3$  is a bounded Lipschitz domain with boundary  $\partial\Omega = \Gamma_m \cup \Gamma_e$ .

### 2.1. Variational Formulation for the Helmholtz Equation for Isotropic Medium with Microinclusions

We define  $\Omega$  as 3D heterogeneous domain with Lipschitz-continuous boundary  $\Gamma$ . Let's introduce the following spaces [4]

$$\mathbf{H}(\operatorname{curl}, \Omega) = \left\{ \mathbf{u} \in \mathbf{L}^2(\Omega) \mid \operatorname{curl} \mathbf{u} \in \mathbf{L}^2(\Omega) \right\}, \quad (4)$$

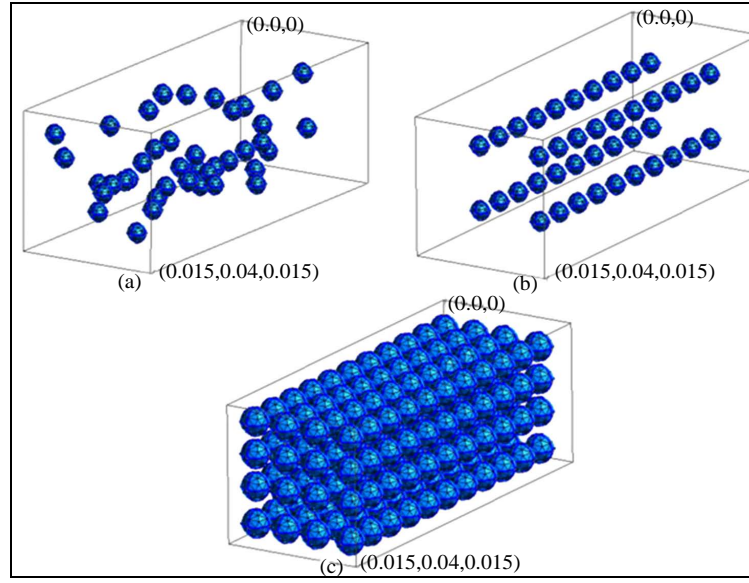


Figure 1. The types of computational domains.

$$H_0(\text{curl}, \Omega) = \left\{ \mathbf{u} \in H(\text{curl}, \Omega) \mid \mathbf{u} \times \mathbf{n} \Big|_{\partial\Omega} = 0 \right\}. \quad (5)$$

The norm in the space  $H(\text{curl}, \Omega)$  is the following:

$$\|\mathbf{u}\|_{H(\text{curl}, \Omega)}^2 = \int_{\Omega} \mathbf{u} \cdot \mathbf{u} d\Omega + \int_{\Omega} \text{curl} \mathbf{u} \cdot \text{curl} \mathbf{u} d\Omega.$$

The special relations called the De Rham complex are fulfilled for the spaces  $H^1(\Omega)$ ,  $H(\text{curl}, \Omega)$ ,  $H(\text{div}, \Omega)$  [18] [19]:

$$H^1(\Omega) \xrightarrow{\text{grad}} H(\text{curl}, \Omega) \xrightarrow{\text{curl}} H(\text{div}, \Omega) \xrightarrow{\text{div}} L^2(\Omega)$$

where

$$H(\text{div}, \Omega) = \left\{ \mathbf{u} \in [L^2(\Omega)]^3 \mid \text{div} \mathbf{u} \in L^2(\Omega) \right\}.$$

The finite-dimensional discrete analogues of the functional spaces also fulfilled the De Rham complex.

The variational formulation for the Equation (1) with boundary conditions (2) and (3) is the following [20]: find  $\mathbf{E} \in H_0(\text{curl}, \Omega)$  such, that  $\forall \mathbf{v} \in H_0(\text{curl}, \Omega)$  the following equation is fulfilled:

$$\int_{\Omega} \mu^{-1} \text{curl} \mathbf{E} \cdot \text{curl} \mathbf{v} d\Omega + \int_{\Omega} k^2 \mathbf{E} \cdot \mathbf{v} d\Omega = 0. \quad (6)$$

The computational domain breaks to  $n$  non-overlapping tetrahedrons (the adaptive triangulation) to obtain the discrete variational formulation. Let us introduce the finite-dimension subspace for the space  $H_0(\text{curl}, \Omega)$

$$H_0^h(\text{curl}, \Omega) \subset H_0(\text{curl}, \Omega). \quad (7)$$

The basic functions  $\mathbf{w}_i^k \in H_0^h(\text{curl}, \Omega)$  are vector functions of the first order. The using of these functions is guaranteed the tangential continuous of  $\mathbf{E}$  on the boundaries between different media [4].

The discrete variational formulation is follow: find  $\mathbf{E}^h \in H_0^h(\text{curl}, \Omega)$  such, that  $\forall \mathbf{v}^h \in H_0^h(\text{curl}, \Omega)$  the following equation is fulfilled:

$$\int_{\Omega} \mu^{-1} \text{curl} \mathbf{E}^h \cdot \text{curl} \mathbf{v}^h d\Omega + \int_{\Omega} k^2 \mathbf{E}^h \cdot \mathbf{v}^h d\Omega + \int_{\partial\Omega} (\mu^{-1} \text{curl} \mathbf{E}^h \times \mathbf{n}) \cdot \mathbf{v}^h d\Omega = 0. \quad (8)$$

The finite element solution of  $\mathbf{E}$  is the following expansion by basic functions:

$$\mathbf{E}^h(\mathbf{x}) = \sum_i q_i \mathbf{w}_i^h(\mathbf{x}) \quad (9)$$

where  $q_i$ —the weights of the expansion  $\mathbf{E}^h$  by basic functions of the space  $\mathbf{H}_0^h(\text{curl}, \Omega)$ .

For test functions  $\mathbf{v}^h = \mathbf{w}_j^h(\mathbf{x})$ ,  $j=1, \dots, N$ , the discrete variational formulation in matrix form is the following:

$$(\mu^{-1}\mathbf{G} + k^2\mathbf{B})\mathbf{q} = \mathbf{F} \quad (10)$$

The elements of the matrixes  $\mathbf{G}$  and  $\mathbf{B}$  are defined as:

$$[\mathbf{G}]_{i,j} = \int_{\Omega_k} \text{curl} \mathbf{w}_i^k \cdot \text{curl} \mathbf{w}_j^k d\Omega_k \quad (11)$$

$$[\mathbf{B}]_{i,j} = \int_{\Omega_k} \mathbf{w}_i^k \cdot \mathbf{w}_j^k d\Omega_k \quad (12)$$

The boundary conditions (2) and (3) are fulfilled in the vector  $\mathbf{F}$ . The system of linear algebraic Equations (10) is solved by the special two-level solver [21].

## 2.2. Variational Formulation for the Helmholtz Equation for Anisotropic Medium with Effective Coefficient

The electric field in frequency domain with effective coefficient is described by the Helmholtz equation:

$$\text{curl} \mu^{-1} \text{curl} \mathbf{E} + i\omega \mathbf{Z} \mathbf{E} = 0, \quad (13)$$

where  $\mathbf{Z}$ —effective coefficient (tensor of the second rank). The boundary conditions (2) and (3) are used.

The functional spaces where we'll find the solution are the same as for isotropic problem (4) and (5).

The variational formulation for anisotropic problem has the following form [17]: find  $\mathbf{E} \in \mathbf{H}_0(\text{curl}, \Omega)$  such that  $\forall \mathbf{W} \in \mathbf{H}_0(\text{curl}, \Omega)$  the following equation is true

$$\int_{\Omega} \mu^{-1} \text{curl} \mathbf{E} \cdot \text{curl} \mathbf{W} d\Omega + \int_{\Omega} i\omega \mathbf{Z} \mathbf{E} \cdot \mathbf{W} d\Omega + \int_{\partial\Omega} (\mu^{-1} \text{curl} \mathbf{E} \times \mathbf{n}) \cdot \mathbf{W} d\Omega = 0 \quad (14)$$

By using the functional spaces (4) and (5) and expansion (9) the variational formulation (14) became the system of linear algebraic equations:

$$\mathbf{A} \mathbf{e}^n + i\omega \mathbf{S} \mathbf{e}^n = \mathbf{F}, \quad (15)$$

where  $\mathbf{A}$ ,  $\mathbf{S}$ —finite-element matrixes defined by the following expressions

$$[\mathbf{A}]_{i,j} = \int_{\Omega_k} \mu^{-1} \text{curl} \mathbf{W}_i \cdot \text{curl} \mathbf{W}_j d\Omega_k$$

$$[\mathbf{S}]_{i,j} = \int_{\Omega_k} \mathbf{W}_i \cdot \mathbf{Z}_k \cdot \mathbf{W}_j d\Omega_k$$

In common case the arbitrary anisotropic medium is described by the following bilinear form:

$$\begin{aligned} \mathbf{Z} = & Z_{xx} \hat{e}_1 \hat{e}_1 + Z_{xy} \hat{e}_1 \hat{e}_2 + Z_{xz} \hat{e}_1 \hat{e}_3 + Z_{yx} \hat{e}_2 \hat{e}_1 + Z_{yy} \hat{e}_2 \hat{e}_2 \\ & + Z_{yz} \hat{e}_2 \hat{e}_3 + Z_{zx} \hat{e}_3 \hat{e}_1 + Z_{zy} \hat{e}_3 \hat{e}_2 + Z_{zz} \hat{e}_3 \hat{e}_3, \end{aligned} \quad (16)$$

For such media the matrix  $\mathbf{S}$  is the following:

$$\begin{aligned}
S_{ij} = & \int_{\Omega_k} Z_{xx} (\hat{e}_1 \cdot \mathbf{W}_i) (\hat{e}_1 \cdot \mathbf{W}_j) d\Omega_k + \int_{\Omega_k} Z_{xy} (\hat{e}_1 \cdot \mathbf{W}_i) (\hat{e}_2 \cdot \mathbf{W}_j) d\Omega_k \\
& + \int_{\Omega_k} Z_{xz} (\hat{e}_1 \cdot \mathbf{W}_i) (\hat{e}_3 \cdot \mathbf{W}_j) d\Omega_k + \int_{\Omega_k} Z_{yx} (\hat{e}_2 \cdot \mathbf{W}_i) (\hat{e}_1 \cdot \mathbf{W}_j) d\Omega_k \\
& + \int_{\Omega_k} Z_{yy} (\hat{e}_2 \cdot \mathbf{W}_i) (\hat{e}_2 \cdot \mathbf{W}_j) d\Omega_k + \int_{\Omega_k} Z_{yz} (\hat{e}_2 \cdot \mathbf{W}_i) (\hat{e}_3 \cdot \mathbf{W}_j) d\Omega_k \\
& + \int_{\Omega_k} Z_{zx} (\hat{e}_3 \cdot \mathbf{W}_i) (\hat{e}_1 \cdot \mathbf{W}_j) d\Omega_k + \int_{\Omega_k} Z_{zy} (\hat{e}_3 \cdot \mathbf{W}_i) (\hat{e}_2 \cdot \mathbf{W}_j) d\Omega_k \\
& + \int_{\Omega_k} Z_{zz} (\hat{e}_3 \cdot \mathbf{W}_i) (\hat{e}_3 \cdot \mathbf{W}_j) d\Omega_k.
\end{aligned} \tag{17}$$

### 3. The Calculation of the Effective Coefficient of the Medium

Let's consider the system of Maxwell equations in frequency domain:

$$\operatorname{curl} \mathbf{E} = -i\omega\mu\mathbf{H}, \tag{18}$$

$$\operatorname{curl} \mathbf{H} = (i\omega\varepsilon + \sigma)\mathbf{E}. \tag{19}$$

The media considered in this work has homogeneous magnetic properties. The coefficient  $i\omega\varepsilon + \sigma$  which includes the information about the microinclusions can be replaced by effective tensor. Let's denote the effective tensor by  $Z$ . So we have the following problem in terms of the second order equation:

$$\operatorname{curl} \mu^{-1} \operatorname{curl} \mathbf{E} + i\omega Z \mathbf{E} = 0, \tag{20}$$

where  $Z$ —complex-valued tensor of the second rank.

The dense tensor of the second rank  $Z$  has the following form

$$Z = \begin{bmatrix} z_{11} & z_{12} & z_{13} \\ z_{21} & z_{22} & z_{23} \\ z_{31} & z_{32} & z_{33} \end{bmatrix}. \tag{21}$$

We use the Equation (19) for the calculation of the  $Z$  components.  $\mathbf{E}$  and  $\operatorname{curl} \mathbf{H}$  are vector variables. That's why we define the following procedure of the computation of the tensor  $Z$ .

$$\begin{aligned}
\|\operatorname{curl} \mathbf{H}\|_{\mathbf{L}^2(\Omega)} &= \|Z\mathbf{E}\|_{\mathbf{L}^2(\Omega)}, \\
\|\operatorname{curl} \mathbf{H}\|_{\mathbf{L}^2(\Omega)} &< \|Z\|_{\mathbf{L}^2(\Omega)} \cdot \|\mathbf{E}\|_{\mathbf{L}^2(\Omega)}.
\end{aligned}$$

where  $\|\cdot\|_{\mathbf{L}^2(\Omega)}$  is the Euclidean norm of the space  $\mathbf{L}^2(\Omega)$ .

The vectors  $\mathbf{H}$  and  $\mathbf{E}$  have three components  $\mathbf{E} = (E_x, E_y, E_z)$ ,  $\operatorname{curl} \mathbf{H} = (\tilde{H}_x, \tilde{H}_y, \tilde{H}_z)$ . So the components of  $Z$  can be computed as

$$Z_{ij} = \|\tilde{H}_i\|_{\mathbf{L}^2(\Omega)} / \|E_j\|_{\mathbf{L}^2(\Omega)}, \tag{22}$$

where  $i, j$  are defined as  $x, y, z$ .

Taking into account that  $\mathbf{E}$  and  $\mathbf{H}$  are the complex-valued vectors, the real and the imaginary components of  $Z$  can be computed separately as

$$\begin{aligned}
\operatorname{Re}(Z_{ij}) &= \|\operatorname{Re}(\tilde{H}_i)\|_{\mathbf{L}^2(\Omega)} / \|\operatorname{Re}(E_j)\|_{\mathbf{L}^2(\Omega)}, \\
\operatorname{Im}(Z_{ij}) &= \|\operatorname{Im}(\tilde{H}_i)\|_{\mathbf{L}^2(\Omega)} / \|\operatorname{Im}(E_j)\|_{\mathbf{L}^2(\Omega)}.
\end{aligned}$$

Another approach to the computation of the effective coefficient as a dense tensor can be proposed. We obtain

the value of the vectors  $\text{curl } \mathbf{H}$  and  $\mathbf{E}$  at the  $n$  points of the domain from the solution of the problem in isotropic media with inclusions. Denote the value of the field at the point  $x_i$  by  $\mathbf{E}(x_i)$ . Then we need to solve the following system to obtain the coefficients of the tensor  $Z$ :

$$\begin{bmatrix} E_x(x_i) & E_y(x_i) & E_z(x_i) \\ E_x(x_j) & E_y(x_j) & E_z(x_j) \\ E_x(x_k) & E_y(x_k) & E_z(x_k) \end{bmatrix} \begin{bmatrix} z_{l1} \\ z_{l2} \\ z_{l3} \end{bmatrix} = \begin{bmatrix} \tilde{H}_l(x_i) \\ \tilde{H}_l(x_j) \\ \tilde{H}_l(x_k) \end{bmatrix}, \quad (23)$$

where  $x_i, x_j, x_k$  are different points in the domain,  $l$  is the number of the tensor's row,  $\tilde{H}_l(x_i)$ —the first, the second or the third component of the vector  $\text{curl } \mathbf{H}$  in the point  $x_i$ . The effective tensor of the medium can be obtained by the averaging of the system's solutions by all the points.

### 4. Numerical Experiments

We choose domain with small spherical inclusions as a computation domain. The inclusions can be located nonregularly (Figure 1(a)), regularly (Figure 1(b)) and we have the domain with large number of inclusions (Figure 1(c)). The size of the computational domain is 15 mm × 40 mm × 15 mm. The diameter of the inclusion is 2 mm. The number of inclusions is 40. The medium is nonmagnetic and  $\mu = \mu_0$  for all cases.

The field source is given electric boundary condition (2) on the faces of the computational domain (Figure 2). The one-side boundary condition is assigned on the left face of the object ( $x=0$ ) and it looks like  $\mathbf{E}_0 = (0, 0, 1)$  (Figure 2(a)).

The boundary conditions (2) assigned on the left ( $x=0$ ), right ( $x=0.015$  mm), top ( $z=0$ ) and bottom ( $z=0.015$  mm) faces of the object make a closed path (Figure 2(b)).

The all tests were done on two frequencies: the low frequency (10 kHz) and high frequency (7 GHz). The wavelength on the low frequency is much more than the inclusion and domain sizes. The wavelength on the high frequency is comparable with the domain size, but much more than the inclusion size.

In the Section 4.1 we estimate the results of the calculation of the coefficient  $Z$  by the formulas (22), (23) in homogeneous medium and in the medium with microinclusions. In the Section 4.2 we try to find the possible values of the medium properties for computing coefficient  $Z$  correctly. The modeling results in the domains with regularly located and nonregularly located inclusions are given in the Section 4.3. The numerical experiments were done on the low (10 kHz) and high (7 GHz) frequencies. Two types of boundary conditions were used. It was one-side boundary condition and conditions assigned on the closed path.

#### 4.1. How to Calculate $Z$ Physically Correctly?

To obtain which approach to find tensor coefficient is correct we define the follow criterion. The components of the electromagnetic field computed for the medium with microinclusions and for the medium with effective

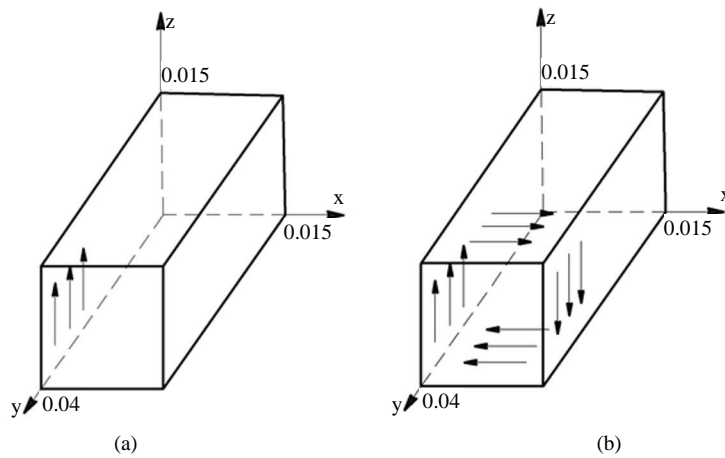


Figure 2. The boundary conditions assigned: (a) on the face; (b) on closed path.

anisotropic coefficient should be in close agreement for correctly computed  $Z$ . We compare the field components extracted by the line passing through the centers of the regularly located inclusions.

The problems in the homogeneous domain without inclusions have been solved. The effective anisotropic coefficients for these cases have been computed. Correctly computed tensor of effective characteristic have to be diagonal with the equal values on the diagonal line. The value of the diagonal coefficients is defined by electro-physical properties of the medium and the source frequency.

The effective coefficients  $Z$  were calculated for homogeneous medium with the conductivity  $\sigma = 0.001 \text{ S/m}$  and the permeability  $\varepsilon = 4.5\varepsilon_0$ .

The formula (22) on the frequency 10 kHz gives:

$$Z^1 = \begin{bmatrix} 0.001 & 5.352E-8 & 0.001 \\ 1.868E+1 & 0.001 & 1.869E+1 \\ 9.999E-4 & 5.352E-8 & 0.001 \end{bmatrix} + i \begin{bmatrix} 9.293E-2 & 9.328E-4 & 9.294E-2 \\ 9.963E-2 & 0.001 & 9.963E-2 \\ 9.385E-2 & 9.42E-4 & 9.386E-2 \end{bmatrix}. \quad (24)$$

And on the frequency 7 GHz:

$$Z^2 = \begin{bmatrix} 2.103E-3 & 1.880E-6 & 2.112E-3 \\ 3.987 & 3.563E-3 & 4.004 \\ 2.096E-3 & 1.873E-6 & 2.105E-3 \end{bmatrix} + i \begin{bmatrix} 2.701E+3 & 1.425E & 2.710E+3 \\ 2.130E+6 & 1.124E+3 & 2.137E+6 \\ 2.690E+3 & 1.419E & 2.699E+3 \end{bmatrix}. \quad (25)$$

The tensors obtained by (22) are dense tensors without predominant of the diagonal elements. The non-diagonal elements of the second row of the tensor are bigger than the all other elements of the tensor. We have a good coincidence between problem with isotropic coefficients and problem with anisotropic coefficient  $Z$  on the frequency 10 kHz (**Figure 3(a)**). But we couldn't obtain results on the frequency 7 GHz. The discrepancy of the problem in the iterative solver has exponentially growth. The solution can't be obtained.

The formula (23) on the frequency 10 kHz gives:

$$Z^3 = \begin{bmatrix} 1e-3 & 9.023e-21 & -2.297e-26 \\ 1.91e-21 & 1e-3 & 3.404e-27 \\ -3.007e-16 & -1.62e-15 & 1e-3 \end{bmatrix} + i \begin{bmatrix} 2.502e-6 & 1.457e-21 & -1.196e-26 \\ -6.404e-21 & 2.502e-6 & 2.8e-26 \\ -1.25e-16 & 5.38e-16 & 2.502e-6 \end{bmatrix}. \quad (26)$$

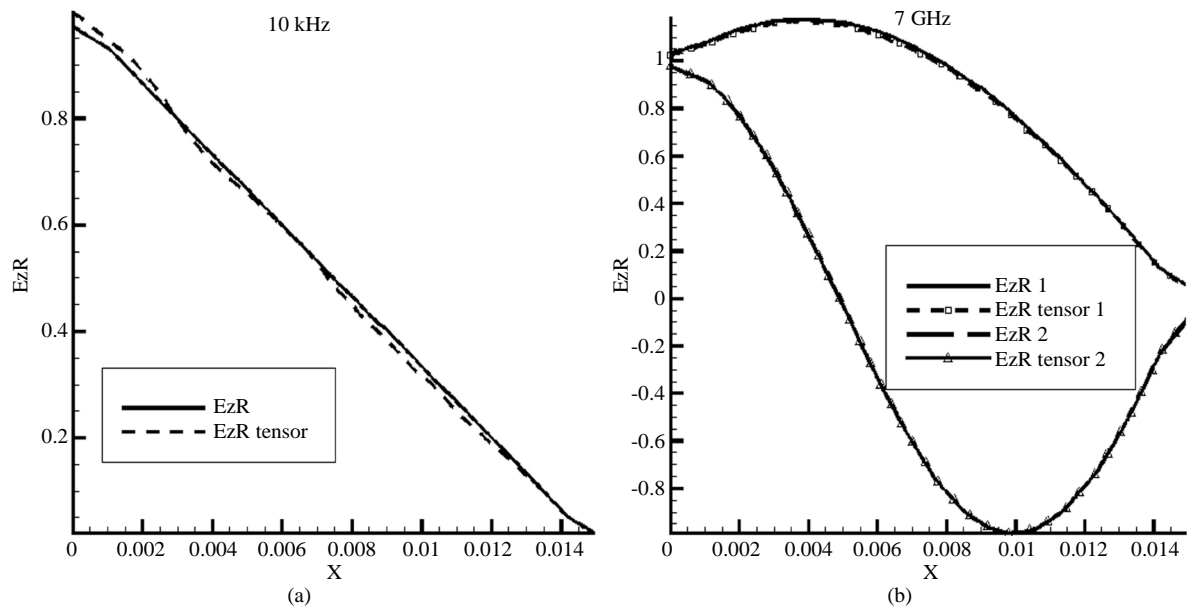


**Figure 3.** The results of the electromagnetic field modeling for homogeneous media on the (a) 10 kHz; (b) 7 GHz. EzR, EzR1 is the real component of the field E for  $\sigma = 0.001 \text{ S/m}$ , EzR2 is the real component of the field for  $\sigma = 0.1 \text{ S/m}$ , EzR tensor is the real component of the field for the problem with anisotropic coefficient.

And on the frequency 7 GHz:

$$Z^4 = \begin{bmatrix} 1e-3 & 1.405e-16 & 2.322e-20 \\ 5.211e-18 & 1e-3 & 1.001e-20 \\ -1.824e-14 & -1.567e-13 & 1e-3 \end{bmatrix} + i \begin{bmatrix} 1.7516 & 1.7957e-16 & -2.843e-20 \\ -9.857e-18 & 1.7516 & 2.353e-21 \\ 4.418e-14 & 4.998e-13 & 1.7516 \end{bmatrix}. \quad (27)$$

The tensors  $Z^3$ ,  $Z^4$  have diagonal predomination. The values of the diagonal elements are equal to the values of the isotropic coefficients  $\sigma$  and  $\omega\epsilon$ . The results of the modeling with these tensors have a good coincidence with the results of the problem with microinclusions for the all frequencies (Figure 3(b)). The same picture is observed for the medium with higher conductivity  $\sigma = 0.1\text{S/m}$  (Figure 3(b)).

The tensor obtained by the (22) for the problem with microinclusions on the low frequency gives the same good result as in homogeneous medium. The values of the field components have a good coincidence outside of the inclusions for the problem with inclusions and the problem with anisotropic coefficient (Figures 4(a) and 5(a)). The solution of the problem with anisotropic coefficient on the high frequency was not obtained for such tensor.

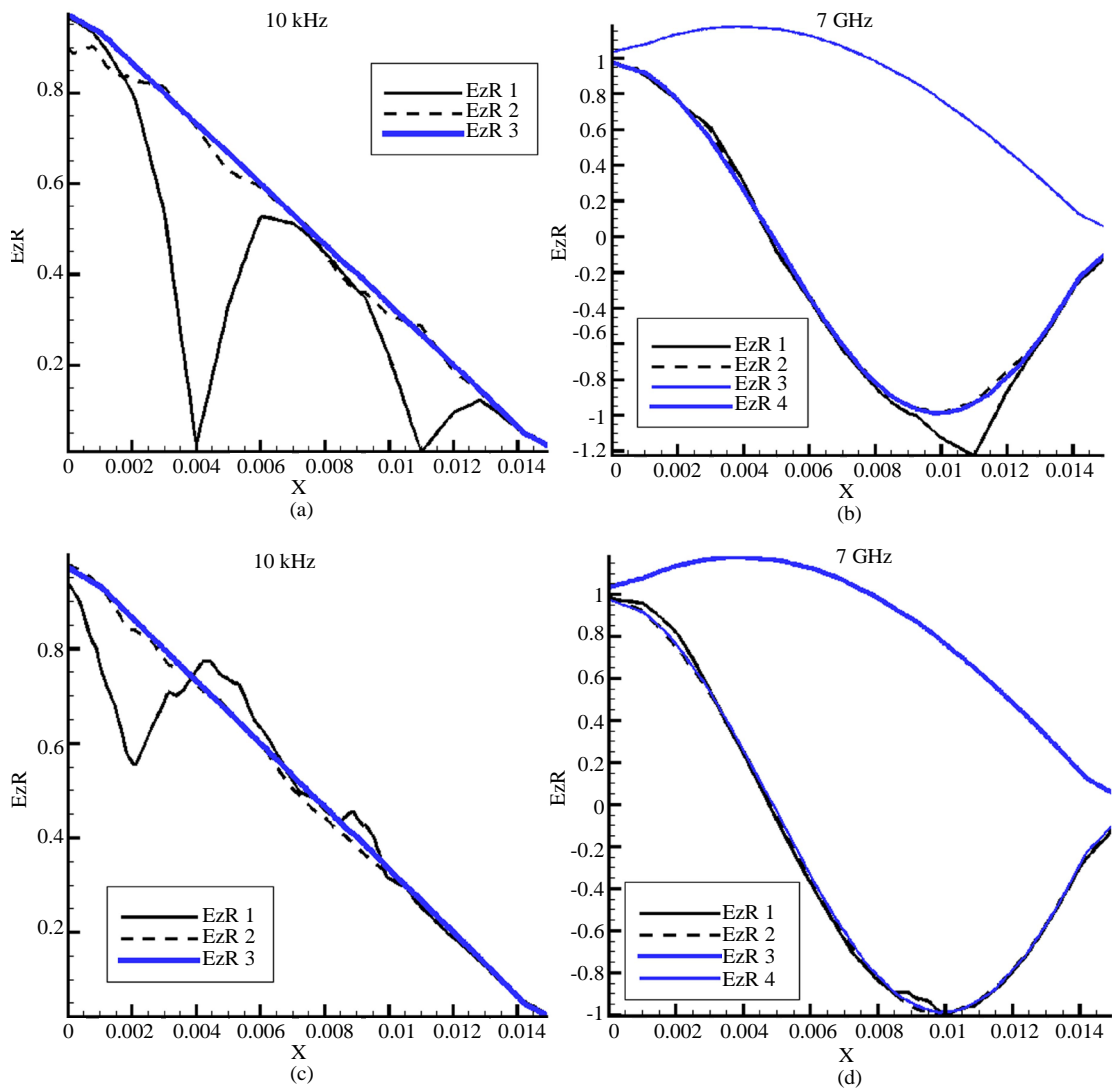


**Figure 4.** The real component of the field  $E_z$  in isotropic medium (EzR1) and anisotropic medium (EzR2) for the frequency 10 kHz ((a), (c)) and frequency 7 GHz ((b), (d)). The boundary condition is on one face. The inclusions location is regular ((a), (b)) and nonregular ((c), (d)). EzR3, EzR4 are the results in homogeneous medium with  $\sigma = 0.1\text{ S/m}$  and  $\sigma = 0.001\text{ S/m}$  respectively.

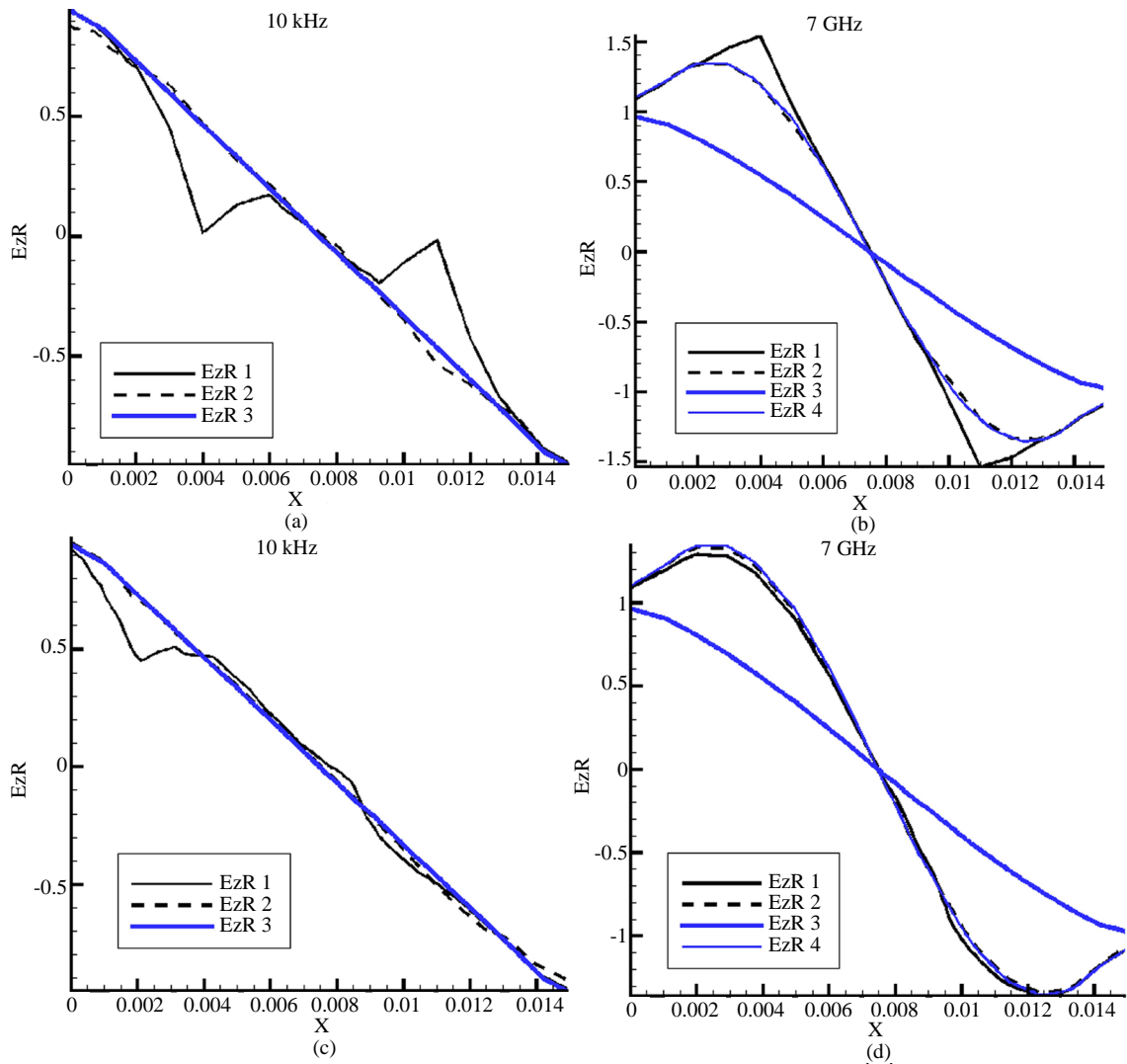


**Figure 5.** The real component of the field  $E_z$  in isotropic medium ( $E_{zR1}$ ) and anisotropic medium ( $E_{zR2}$ ) for the frequency 10 kHz ((a), (c)) and frequency 7 GHz ((b), (d)). The boundary conditions are done by closed path. The inclusion location is regular (a), (b) and non regular ((c), (d)).  $E_{zR3}$ ,  $E_{zR4}$  are the results in homogeneous medium with  $\sigma = 0.1$  S/m and  $\sigma = 0.001$  S/m respectively.

The tensors obtained by (23) allow getting solution of the problem with anisotropic coefficient for the medium with inclusions on the all frequencies. We have a good coincidence between the results of these problems outside of the inclusions. (Figures 4 and 5). The results given later are obtained using the formula (23).

#### 4.2. The Admitted Region for the Parameters of the Inclusions

Effective coefficient is some average of the medium consisted from the materials with different properties. In this Section we define for what kind of media proposed approach can be used.

The series of the numerical experiments have been done to obtain the possible contrast between properties of the matrix of the object and inclusions. The conductivity of the matrix is equal  $\sigma = 0.001$  S/m for the all experiments (Figure 1(b)). The conductivity of the inclusions changes from  $\sigma = 0.1$  S/m till  $\sigma = 1000$  S/m. The results of the modeling for the problem with microinclusions are presented in the Figure 6(a). You can see that the behavior of the field inside the inclusion is changed by increasing the conductivity since  $\sigma = 10$  S/m. We can solve the problem with isotropic coefficients in the medium with microinclusions even for the contrast between the matrix and the inclusion equal to  $10^6$ .

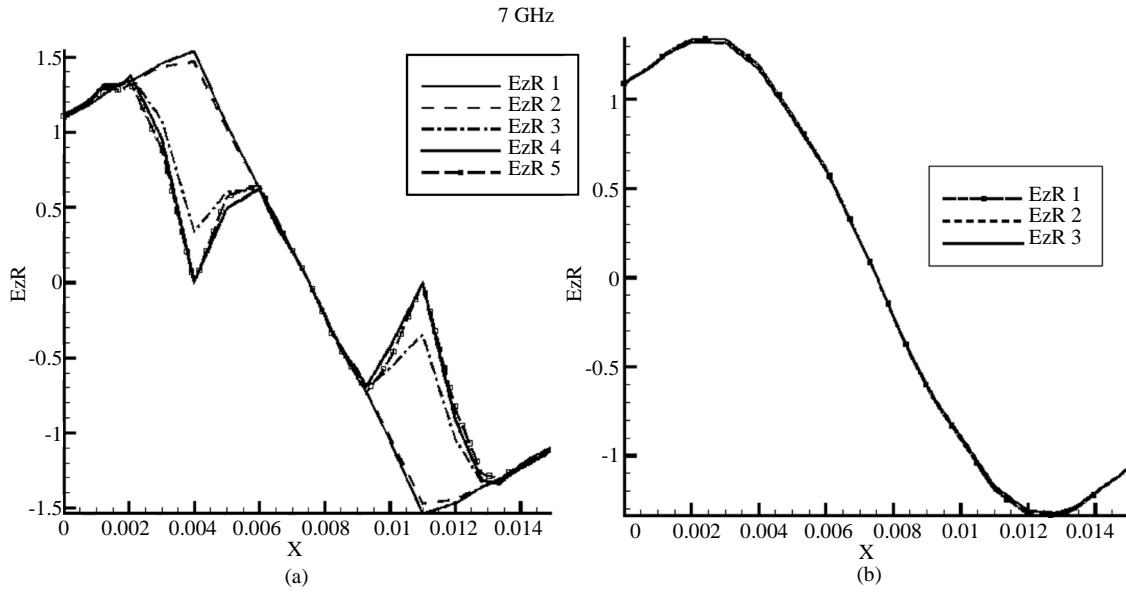


**Figure 6.** The real field component  $E_z$  for the different conductivity of the inclusions. The matrix conductivity  $\sigma = 0.001$  S/m, the inclusion conductivity 1 –  $\sigma = 0.1$  S/m, 2 –  $\sigma = 1$  S/m, 3 –  $\sigma = 10$  S/m, 4 –  $\sigma = 100$  S/m, 5 –  $\sigma = 1000$  S/m.

This is not true for the problem with anisotropic coefficient. The solutions of the problem with anisotropic coefficient have been obtained only for the first three cases. The contrast for these problems is 100, 1000 and 10000 (**Figure 6(b)**). The modeling results have low difference between each other. We have smooth picture which is close to the results in the homogeneous medium with the conductivity of the object’s matrix. The graph for the contrast equal to 10000 has a little bit lower amplitude inside the inclusion than other. The tensors for the higher values of the contrast don’t allow getting the solution because of non-stable work of the iterative solver.

The inclusions occupies about 2% from the all object’s volume for the domain with regularly located inclusions (**Figure 1(b)**). We suppose that the properties of the object’s matrix are dominant in the averaging procedure when we compute tensor coefficient because of little volume of the inclusions. We increase the number of the inclusion to prove it. Next problem have 176 spherical inclusions. The diameter of the sphere is 3 mm. The volume of the all inclusions is equal to 27% from the all object volume (**Figure 1(c)**). The tensor  $Z$  for this problem on the frequency 10 kHz is the following:

$$Z^3 = \begin{bmatrix} 2.75e-2 & 1.05e-5 & -5.53e-7 \\ 3.49e-8 & 2.75e-2 & 1.25e-8 \\ 1.19e-7 & 2.57e-6 & 2.75e-2 \end{bmatrix} + i \begin{bmatrix} 1.98e-6 & -7.92e-10 & -1.24e-10 \\ 1.05e-11 & 1.98e-6 & 1.56e-11 \\ -2.3e-10 & -1.33e-9 & 1.98e-6 \end{bmatrix}. \quad (28)$$

And on the frequency 7 GHz:

$$Z^4 = \begin{bmatrix} 2.75e-2 & 3.09e-5 & -3.64e-6 \\ -6.35e-8 & 2.75e-2 & -1.86e-7 \\ -3.97e-7 & 1.5e-5 & 2.75e-2 \end{bmatrix} + i \begin{bmatrix} 1.39 & -7.68e-5 & 2.24e-5 \\ 3.82e-7 & 1.39 & 6.71e-7 \\ 6.56e-6 & -2.13e-4 & 1.39 \end{bmatrix}. \quad (29)$$

We can see in the **Figure 7(a)** that the electromagnetic field for the problem with effective coefficient is the same as in homogeneous medium for the frequency 10 kHz. More strong interaction between inclusions appears on the high frequency. The graph of the real field component  $E_z$  for the problem with tensor coefficient are situated between the graphs obtained for the homogeneous media with the conductivities equal to the conductivity of matrix and inclusions. The form of the graph line is close to the form of the graph for homogeneous medium. We assume that the behavior of the field propagation changes for the object with large number of close situated inclusions. In this case the effect of anisotropy is appeared.

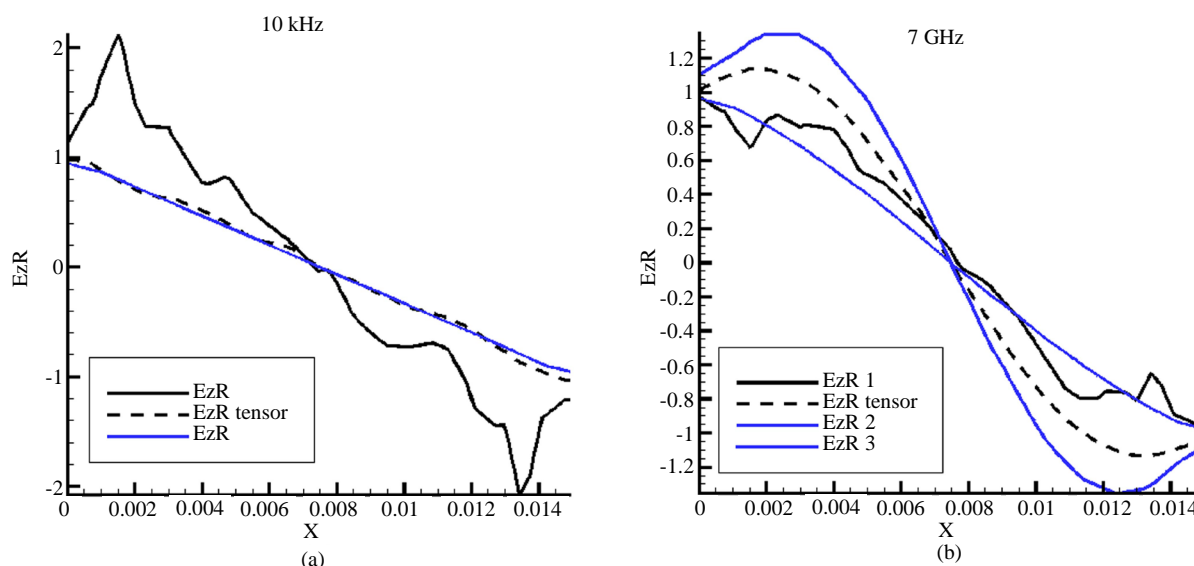


**Figure 7.** The real component of the field  $E_z$  for the frequency 10 kHz (a) and frequency 7 GHz (b).  $E_zR1$  is the result for the problem with large number of inclusions,  $E_zR$  tensor is the result for the problem with tensor  $Z$ .  $E_zR2$ ,  $E_zR3$  is the result for the problem in homogeneous medium with the conductivities  $\sigma = 0.001$  S/m and  $\sigma = 0.1$  S/m respectively.

### 4.3. The Results of the Modeling of Objects with Microinclusions

We investigate the influence of the boundary conditions and inclusions location on the electromagnetic field in this Section. Two cases of the inclusions location are considered. The first case is the regular location of the 40 inclusions (Figure 1(b)). The second case is the nonregular location of 40 inclusions without overlapping (Figure 1(a)). The one-side boundary conditions and conditions on the closed path are used for each case. The used frequencies are 10 kHz and 7 GHz. You can see the graphs of the electromagnetic field component for the problem in the isotropic medium with microinclusions and for the problem with tensor coefficient in the Figures 4 and 5. Also we add to the figures the graphs for homogeneous media with the conductivities equal to the conductivity of the object's matrix and inclusions. The graphs for the cases with the regularly located inclusions are made by the lines passing through the centers of inclusions. The line for the graph in case of nonregular inclusions is chosen as a nearest to the maximum concentration of the inclusions.

The microinclusions located near the face with boundary condition can be distinguished more clearly for the domain with regular located inclusions on the low frequency. We can't choose the line passed though more than one inclusion for the domain with nonregular location of the inclusion. So the influence of inclusions on the field poorly expresses on the graphs. The maximum distortion is located near the face with boundary condition for low frequency. The distortion of the real component of the field  $E_z$  became less visible on the high frequency for the all cases.

The results for the problems in anisotropic medium have a minimal distortion for the all frequencies and inclusion locations in comparison with the problem in homogeneous medium with the matrix conductivity.

We can distinguish the inclusions in the problem with the boundary conditions on the closed path for the all frequencies (Figure 5). The results for the problem in the anisotropic medium have a good coincidence to the results for the problem in isotropic medium with microinclusions outside the inclusions. The distortion of the graph for nonregular location of the inclusions is larger on the left side of the object because there are more inclusions located (Figure 5(c)). The influence of the inclusions on the high frequency is non-significant and the form of the field is close to the distribution in the homogeneous medium.

## 5. Conclusions

The new approach to the calculation of the effective anisotropic characteristic of the medium with microinclusions is proposed in this work. The limits of using such approach are investigated. The modeling results for the problem with anisotropic coefficient are compared with the results of the problem in isotropic medium with mi-

croinclusions. We analyzed the influence from the inclusion location (regular/nonregular) to the computed tensor.

Proposed procedure of calculating effective tensor characteristic of the medium is verified by the results of the modeling problem in the media with isotropic coefficients. We find the limits of possible contrast of the object's matrix and inclusion properties. The possible contrast can be no more than  $10^4$ . The proposed approach doesn't have limits on inclusion location, type of boundary condition or frequency.

## References

- [1] Soukoulis, C.M. and Wegener, M. (2011) Past Achievements and Future Challenges in the Development of Three-Dimensional Photonic Metamaterials. *Nature Photonics*, **5**, 523-530.
- [2] Smith, D.R. and Kroll, N. (2000) Negative Refractive Index in Left-Handed Materials. *Physical Review Letters*, **85**, 2933-2936. <http://dx.doi.org/10.1103/PhysRevLett.85.2933>
- [3] Li, J. and Huang, Y. (2013) Introduction to Metamaterials. *Time-Domain Finite Element Methods for Maxwell's Equations in Metamaterials*, Springer, Berlin.
- [4] Nédélec, J.-C. (1980) Mixed Finite Elements in  $R^3$ . *Numerische Mathematik*, **35**, 315-341. <http://dx.doi.org/10.1007/BF01396415>
- [5] Nédélec, J.-C. (1986) A New Family of Mixed Finite Elements in  $R^3$ . *Numerische Mathematik*, **50**, 57-81. <http://dx.doi.org/10.1007/BF01389668>
- [6] Lanteri, S. and Scheid, C. (2013) Convergence of a Discontinuous Galerkin Scheme for the Mixed Time-Domain Maxwell's Equations in Dispersive Media. *IMA Journal of Numerical Analysis*, **33**, 432-459.
- [7] Hesthaven, J.S. and Warburton, T. (2004) High-Order Nodal Discontinuous Galerkin Methods for the Maxwell Eigenvalue Problem. *Philosophical Transactions of the Royal Society of London. Series A: Mathematical, Physical and Engineering Sciences*, **362**, 493-524.
- [8] Shelby, R.A., Smith, D.R., Nemat-Nasser, S.C. and Schultz, S. (2001) Microwave Transmission through a Two-Dimensional, Isotropic, Left-Handed Metamaterial. *Applied Physics Letters*, **78**, 489-491. <http://dx.doi.org/10.1063/1.1343489>
- [9] Castaneda, P.P. and Willis, J.R. (1995) The Effect of Spatial Distribution on the Effective Behavior of Composite Materials and Cracked Media. *Journal of the Mechanics and Physics of Solids*, **43**, 1919-1951. [http://dx.doi.org/10.1016/0022-5096\(95\)00058-Q](http://dx.doi.org/10.1016/0022-5096(95)00058-Q)
- [10] Hashin, Z. and Shtrikman, Sh. (1962) A Variational Approach to the Theory of the Effective Magnetic Permeability of Multiphase Materials. *Journal of applied Physics*, **33**, 3125-3131. <http://dx.doi.org/10.1063/1.1728579>
- [11] Milton, G.W. and Kohn, R.V. (1988) Variational Bounds on the Effective Moduli of Anisotropic Composites. *Journal of the Mechanics and Physics of Solids*, **36**, 597-629. [http://dx.doi.org/10.1016/0022-5096\(88\)90001-4](http://dx.doi.org/10.1016/0022-5096(88)90001-4)
- [12] Yakhno, V.G., Yakhno, T.M. and Kasap, M. (2006) A Novel Approach for Modeling and Simulation of Electromagnetic Waves in Anisotropic Dielectrics. *International Journal of Solids and Structures*, **43**, 6261-6276. <http://dx.doi.org/10.1016/j.ijsolstr.2005.07.028>
- [13] Yin, Ch. and Weidelt, P. (1999) Geoelectrical Fields in a Layered Earth with Arbitrary Anisotropy. *Geophysics*, **64**, 426-434. <http://dx.doi.org/10.1190/1.1444547>
- [14] Yin, Ch. and Maurer, H.-M. (2001) Electromagnetic Induction in a Layered Earth with Arbitrary Anisotropy. *Geophysics*, **66**, 1405-1416. <http://dx.doi.org/10.1190/1.1487086>
- [15] Loseth, L.O. and Ursin, B. (2007) Electromagnetic Fields in Planarly Layered Anisotropic Media. *Geophysical Journal International*, **170**, 44-80. <http://dx.doi.org/10.1111/j.1365-246X.2007.03390.x>
- [16] Orlovskaya, N.V., Shurina, E.P. and Epov, M.I. (2006) Modeling of Electromagnetic Field in Anisotropic Electroconductive Media. *Computational Technologies*, **11**, 99-116.
- [17] Shtabel, N.V. and Shurina, E.P. (2013) Analysis of Vector Finite Element Approximations of Maxwell's Equations in Anisotropic Media. *Compensation Technologies*, **18**, 91-104.
- [18] Hiptmair, R. and Zheng, W.-Y. (2009) Local Multigrid in H (curl). *Journal of Computational Mathematics*, **27**, 573-603. <http://dx.doi.org/10.4208/jcm.2009.27.5.012>
- [19] Hiptmair, R. (2001) Higher Order Whitney Forms. *Progress in Electromagnetics Research*, **32**, 271-299. <http://dx.doi.org/10.2528/PIER00080111>
- [20] Monk, P. (2003) *Finite Element Methods for Maxwell's Equations*. Oxford University Press, Oxford. <http://dx.doi.org/10.1093/acprof:oso/9780198508885.001.0001>
- [21] Nechaev, O., Shurina, E. and Botchev, M. (2008) Multilevel Iterative Solvers for the Edge Finite Element Solution of the 3D Maxwell Equation. *Computers & Mathematics with Applications*, **55**, 2346-2362. <http://dx.doi.org/10.1016/j.camwa.2007.11.003>